REPORT DOCUMENTATION PAGE

Form Approved OMB NO. 0704-0188

1. REPORT DATE (DD-MM-YYYY)	2. REPORT TYPE	3. DATES COVERED (From - To)
11-10-2018	Final Report	15-Sep-2014 - 14-Aug-2018

4. TITLE AND SUBTITLE
Final Report: Angularly-Resolved Elastic Light Scattering of Atmospheric Particles: Experimental Measurements and Model Verification

5a. CONTRACT NUMBER
W911NF-14-2-0098

5b. GRANT NUMBER

5c. PROGRAM ELEMENT NUMBER
611102

6. AUTHORS

5d. PROJECT NUMBER

5e. TASK NUMBER

5f. WORK UNIT NUMBER

7. PERFORMING ORGANIZATION NAMES AND ADDRESSES
West Chester University of Pennsylvania
700 South High Street

West Chester, PA 19383 -0001

8. PERFORMING ORGANIZATION REPORT NUMBER

9. SPONSORING/MONITORING AGENCY NAME(S) AND ADDRESS (ES)
U.S. Army Research Office
P.O. Box 12211
Research Triangle Park, NC 27709-2211

10. SPONSOR/MONITOR'S ACRONYM(S)
ARO

11. SPONSOR/MONITOR'S REPORT NUMBER(S)
64807-CH.1

12. DISTRIBUTION AVAILIBILITY STATEMENT
Approved for public release; distribution is unlimited.

13. SUPPLEMENTARY NOTES
The views, opinions and/or findings contained in this report are those of the author(s) and should not contrued as an official Department of the Army position, policy or decision, unless so designated by other documentation.

14. ABSTRACT

15. SUBJECT TERMS

16. SECURITY CLASSIFICATION OF:			17. LIMITATION OF ABSTRACT	15. NUMBER OF PAGES	19a. NAME OF RESPONSIBLE PERSON
a. REPORT	b. ABSTRACT	c. THIS PAGE			Kevin Aptowicz
UU	UU	UU	UU		19b. TELEPHONE NUMBER 610-436-3010

RPPR Final Report
as of 02-Jan-2019

Agency Code:

Proposal Number: 64807CH **Agreement Number: W911NF-14-2-0098**
INVESTIGATOR(S):

Name: Kevin Aptowicz
Email: kaptowicz@wcupa.edu
Phone Number: 6104363010
Principal: Y

Organization: **West Chester University of Pennsylvania**
Address: 700 South High Street, West Chester, PA 193830001
Country: USA
DUNS Number: 627341274 EIN: 232417773
Report Date: 14-Nov-2018 Date Received: 11-Oct-2018
Final Report for Period Beginning 15-Sep-2014 and Ending 14-Aug-2018
Title: Angularly-Resolved Elastic Light Scattering of Atmospheric Particles: Experimental Measurements and Model Verification
Begin Performance Period: 15-Sep-2014 **End Performance Period:** 14-Aug-2018
Report Term: 0-Other
Submitted By: Kevin Aptowicz Email: kaptowicz@wcupa.edu
Phone: (610) 436-3010

STEM Degrees: 0 **STEM Participants:** 2

Major Goals: In the grant proposal 64807-EV, five questions were outlined to be explored:

Question 1. To what extent do inversion techniques using the spheroidal model accurately reproduce physical characteristics of atmospheric aerosol?

Question 2. Is the agglomerate-debris-particle model a more accurate representation of particle scattering?

Question 3. How accurate are size measurements of single particles using our apparatus?

Question 4. What features of the scattering patterns can be used to identify the sphericity of the interrogated particle? And how does the scattering phase function evolve with sphericity?

Question 5. If the scattering patterns of individual particles are grouped by features in their scattering phase functions, what insights can be discerned about the physical properties of these particles that lead to the similarities in the scattering phase function?

Accomplishments: This is the fourth year of the grant. It is a no cost extension year. In the first two years of the grant, Jason Zallie and Daniel Landgraf (both undergraduate researchers) performed research exploring the questions outlined in the grant proposal. Jason and Dan both graduated in the Spring of 2017. In the third year, two new undergraduate researchers joined the research effort: Gabe Seymour and Sequoyah Walters. Most of the results discussed below represents the research efforts of Gabe and Sequoyah from the summer of 2017. During the no cost extension year, we have focused on publishing our findings. We recently had one paper accepted into the Journal of Quantitative Spectroscopy and Radiative Transfer with minor edits. We are about to submit another paper. Below is a summary of the progress as it relates to each research question outlined in the grant proposal.

QUESTION #1. To what extent do inversion techniques using the spheroidal model accurately reproduce physical characteristics of atmospheric aerosol?
PROGRESS: During the first two reporting periods, we worked on an auto-correlation technique that would analyze light scattering patterns of single particles and roughly classify them by particle morphology. We applied this technique to our experimentally captured light scattering patterns of atmospheric aerosol particles. In the third reporting period, we further explored this technique by calculating light scattering patterns from simulated particles

and analyzing them. In particular, we were interested in exploring how the light scattering patterns of particles evolve as particles are deformed away from a homogenous sphere. We simulated particles in which we could evolve their morphology from a simple single sphere to a more complex particle. Here are the three types of particles we explored:

Spheroid - The deformation of the spheroid away from a perfect sphere can be tuned by varying the aspect ratio of the spheroid. Starting with an aspect ratio of 1 (a perfect sphere), we both steadily increased (creating a prolate spheroid) and decreased (creating an oblate spheroid) the aspect ratio. As we varied the aspect ratio, we can calculated the scattering patterns of these different particle shapes. This gave us insight into how the overall shape of a particle affects the light scattering pattern.

Chebyshev - The deformation of the Chebyshev particle away from a perfect sphere can be tuned by varying the amplitude of the surface waves. Starting with an amplitude of 0 (a perfect sphere), we steadily increased the amplitude of the surface waves and calculated the scattering patterns of these different particle shapes. This gave us insight into how the surface roughness of the particle affects the light scattering pattern.

Clusters - The final particle shape we explored were clusters of spherical particles inside a large sphere (i.e. an inclusion). If we set the optical properties (i.e. complex refractive index) of the internal spherical particles to that of the large encompassing sphere, the inclusion would become a homogeneous single sphere. Thus, by slowly varying the optical properties of the internal spheres away from the optical properties of the encompassing sphere, we could evolve the particle morphology away from a perfect homogeneous spherical particles to an inclusion. This gave us insight into how the internal homogeneity of the particles affects the light scattering pattern.

For each of this cases, we compared the results of the autocorrelation analysis to the previously results on atmospheric particles. Our preliminary findings suggest that the evolution of spheroidal particles best captures the range of shapes seen in atmospheric aerosol particles. Although not conclusive, this suggests that the key morphological feature that is contributing to diversity of scattering patterns in our atmospheric dataset is particle shape.

QUESTION #2. Is the agglomerate-debris-particle model a more accurate representation of particle scattering?
PROGRESS: We have not yet explored this question.

QUESTION #3. How accurate are size measurements of single particles using our apparatus?
PROGRESS: Building on the progress made during the second reporting period, we continued to explore sizing particles using features in the scattering patterns. However, this research took a interesting turn when we realized that we might be able to extract single-particle absorption from the light scattering patterns. In particular, for each pattern, we can extract information about particle size based on the speckle size. In addition, once we know particle size, the overall scattering intensity of the particle provides insight into the particle absorption. We performed a series of simulations using the optical properties of common aerosol particles (e.g. oceanic, dust, sulfate, and soot) and were able to roughly characterize the particles from their scattering patterns based on their absorptive properties. The results were refined over this past year and submitted to the Journal of Quantitative Spectroscopy and Radiative Transfer for publication.

QUESTION #4: What features of the scattering patterns can be used to identify the sphericity of the interrogated particle? And how does the scattering phase function evolve with sphericity?
PROGRESS: Our progress on this question is discussed in the answer to question #1 above. In particular, we utilized simulated scattering patterns from spheroidal particle, Chebyshev particles, and inclusions to explore the evolution of the scattering pattern as particle morphology was evolved away from a perfect sphere.

QUESTION #5: If the scattering patterns of individual particles are grouped by features in their scattering phase functions, what insights can be discerned about the physical properties of these particles that lead to the similarities in the scattering phase function?
PROGRESS: We have not yet explored this question.

RPPR Final Report
as of 02-Jan-2019

Training Opportunities: Undergraduate Research Mentoring - Through this grant, four undergraduate students (Daniel Landgraf, Jason Zallie, Gabe Seymour, and Sequoyah Walters) have been trained as researchers by the P. I.. Examples of skills honed are: preparing a scientific abstract for a presentation, preparing a scientific poster for presentation, preparing a scientific talk, preparing figures for a journal submission, writing a research journal article, programming in Matlab and Fortran, using software packages such as anaconda for python, inkscape, and latex editor.

Dan and Jason attended the AGU Fall meeting in San Francisco in December of 2016 and 2017. It was an incredible experience for both of them and provided them with an excellent introduction to the culture of science.

Gabe and Sequoyah attended and presented at the Elastic Light Scattering Conference in College Station, Texas, in March of 2018. Their research was very well received.

Over the last reporting period, the PI has worked with Sequoyah Walters and Jason Zallie to publish their results. Their research was submitted to the Journal of Quantitative Spectroscopy and Radiative Transfer and accepted for publication after minor modifications. Sequoyah Walters, an undergraduate student, was the first author on the paper.

RPPR Final Report
as of 02-Jan-2019

Results Dissemination: 2018
Measuring single-particle absorption from elastic light scattering patterns of complex aggregates, S. Walters, J. Zallie, G. Seymour, D. Landgraf, and K. Aptowicz, 17th Conference on Electromagnetic & Light Scattering Elastic Light Scattering Conference, Texas Station, TX, March 4th – 9th, 2018. (S. Walters, a WCU undergraduate, presented poster)

Insights into atmospheric aerosol particle morphology from simulations of single-particle light scattering, G. Seymour, D. Landgraf, R. Pinnick, Y. Pan, and K. Aptowicz, 17th Conference on Electromagnetic & Light Scattering Elastic Light Scattering Conference, Texas Station, TX, March 4th – 9th, 2018. (G. Seymour, a WCU undergraduate, presented poster)

2017
Angularly-Resolved Elastic Light Scattering of Atmospheric Particles, K. Aptowicz, Army Research Office Division Review, Durham, NC, August 7th – 11th, 2017

Insights into particle morphology from single-particle light scattering, D. Landgraf, J. Zallie, R.G. Pinnick, Y.L. Pan, and K.B. Aptowicz, 16th Conference on Electromagnetic & Light Scattering Elastic Light Scattering Conference, College Park, MD, March 19th – 25th, 2017.

2016
Classifying Sphere, Sphere-Like, and Non-Spherical Particles Using Two-Dimensional Angular Optical Scattering (TAOS) Patterns, D. Landgraf, J.T. Zallie, Y. Pan, R.G. Pinnick, and K.B. Aptowicz, American Geophysical Union Fall Meeting, San Francisco, CA, December 12th – 16th, 2016. (D. Landgraf, a WCU undergraduate, presented poster)

Insights Into Particle Morphology From the Autocorrelation Function of Two-Dimensional Angular Optical Scattering (TAOS) Patterns, J.T. Zallie, Y. Pan, R.G. Pinnick, and K.B. Aptowicz, American Geophysical Union Fall Meeting, San Francisco, CA, December 12th – 16th, 2016. (J. T. Zallie, a WCU undergraduate, presented poster)

Single-Particle Morphology from Two-Dimensional Autocorrelation of Angularly?Resolved Light Scattering, K.B. Aptowicz, D. Landgraf, J. Zallie, G. Videen, S. Hill, R. Pinnick, and Y. Pan, American Association of Aerosol Research (AAAR) 35th Annual Conference, Portland, OR, October 17th – October 21st, 2016.

2015
Sizing of individual aerosol particles using TAOS (Two-dimensional Angular Optical Scattering) pattern total intensity, J.T. Zallie, K.B. Aptowicz, S. Martin, and Y. Pan, American Geophysical Union Fall Meeting, San Francisco, CA, December 14th – 18th, 2015. (J. T. Zallie, a WCU undergraduate, presented poster)

Exploring the evolution of the aerosol phase function away from spherical particles using scattering patterns from single atmospheric aerosol particles, D. Landgraf, K.B. Aptowicz, J. Sugar, S. Martin, and Y Pan., American Geophysical Union Fall Meeting, San Francisco, CA, December 14th – 18th, 2015. (D. Landgraf, a WCU undergraduate, presented poster)

Decomposition of atmospheric aerosol phase function by particle size and morphology via single particle scattering measurements, K.B. Aptowicz, Colloquium Presentation, Fordham University, Bronx, NY, March 25th, 2015.

Honors and Awards: 2017 Spotlight on Research Award Recipient from State Senator Dinniman

Protocol Activity Status:

Technology Transfer: There have been close interaction with scientists at the Army Research Laboratories (ARL). ARL scientists Dr. Yong-Le Pan and Dr. Gorden Videen our coauthors on the work submitted with the Journal of Quantitative Spectroscopy and Radiative Transfer.

PARTICIPANTS:

Participant Type: PD/PI
Participant: Kevin Bruce Aptowicz

Person Months Worked: 4.00 **Funding Support:**
Project Contribution:
International Collaboration:
International Travel:
National Academy Member: N
Other Collaborators:

Participant Type: Undergraduate Student
Participant: Jason Zallie
Person Months Worked: 1.00 **Funding Support:**
Project Contribution:
International Collaboration:
International Travel:
National Academy Member: N
Other Collaborators:

Participant Type: Undergraduate Student
Participant: Daniel Landgraf
Person Months Worked: 1.00 **Funding Support:**
Project Contribution:
International Collaboration:
International Travel:
National Academy Member: N
Other Collaborators:

Participant Type: Undergraduate Student
Participant: Sequoyah Walters
Person Months Worked: 4.00 **Funding Support:**
Project Contribution:
International Collaboration:
International Travel:
National Academy Member: N
Other Collaborators:

Participant Type: Undergraduate Student
Participant: Gabriel Seymour
Person Months Worked: 2.00 **Funding Support:**
Project Contribution:
International Collaboration:
International Travel:
National Academy Member: N
Other Collaborators:

RPPR Final Report
as of 02-Jan-2019

Characterizing the size and absorption of single nonspherical aerosol particles from angularly-resolved elastic light scattering

Sequoyah Walters[a], Jason Zallie[a], Gabriel Seymour[a], Yong-Le Pan[b], Gorden Videen[b], Kevin B. Aptowicz[a,*]

[a] *Department of Physics, West Chester University, West Chester, PA 19383, USA*
[b] *US Army Research Laboratory, 2800 Powder Mill Road, Adelphi, MD 20783, USA*

Abstract

Measuring the absorption of a single aerosol particle is a challenging endeavor. Of the few techniques available, none are suitable for measuring the single-particle absorption of coarse-mode nonspherical aerosols. Analysis of two-dimensional angular optical scattering (TAOS) patterns provide a possible pathway to perform this measurement. Using a Multiple-Sphere T-Matrix (MSTM) code, we simulate the captured TAOS patterns with geometries similar to a previously designed instrument. By analyzing the size of the speckle and the integrated irradiance of these simulated TAOS patterns, we are able to distinguish between high-absorbing, weak-absorbing, and non-absorbing particles over the size range of 2 μm to 10 μm. In particular, the speckle present in the scattering patterns provides a means to estimate the size of the particle. Once the size of the particle is known, the integrated irradiance provides insight into the absorption of the particle.

Keywords: Single Particle, Absorption, Elastic Light Scattering, Aerosol

*Corresponding author
Email address: kaptowicz@wcupa.edu (Kevin B. Aptowicz)

1. Introduction

Our atmosphere is composed of absorbing aerosol particles ranging from high-absorbing black carbon to less-absorbing mineral dust and brown carbon [1, 2, 3]. Absorbing aerosol particles affect our Earth's climate as well as pose a risk to public health [4, 5, 6, 7]. As such, monitoring and characterizing the regional and global distribution of these aerosol particulates is of great interest.

Measuring the temporal and spatial distribution of absorbing aerosol particles in our atmosphere requires a multifaceted approach. Although remote sensing using ground stations and satellites is needed for adequate spatial and temporal coverage, in situ measurements in aircraft and at surface stations serve to constrain, improve, and test inversion algorithms [5]. Furthermore, single-particle measurements of absorption provide critical insights that would be lost when performing ensemble measurements [8, 9].

A number of techniques have been described in the literature to measure the absorptive properties of single aerosol particles. Willoughby et al. describe a method in which a particle is heated with laser light and the imaginary component of refractive index is determined by monitoring the angular variation of elastically scattered light [10]. However the analysis is limited to spherical particles. Nakagawa et al. designed a single-particle polar nephelometer that determines the complex refractive index of droplets of an aqueous solution of nigrosine dye by comparing the angular scattering with Mie theory [11]. Again, the analysis of the complex refractive index is limited to spherical particles. Gong et al. utilize an optical trap in combination with cavity ringdown spectroscopy to measure the extinction of light from both spherical and nonspherical single aerosol particles, but the analysis does not delineate between the contributions of absorption and scattering to extinction [12].

An instrument more widely used in field campaigns is the Single Particle Soot Photometer (SP2) [13, 14]. It measures the refractory black carbon mass of individual black carbon particles by laser-induced incandescence [15, 16, 17]. The particle size range for this measurement is approximately 70 to 500 nm mass

equivalent diameter, although it depends upon particle density. In addition to measuring the refractory black carbon mass, the SP2 estimates the particle size by measuring an elastic scattering signal. Moteki et al. used the elastic scattering signal of the SP2 as well as the mass determined from an aerosol particle mass analyzer (APM) to estimate the refractive indices of small nonspherical particles [18]. In particular, when invoking the Raleigh-Gans approximation, the scattering cross-section of small aerosol particles is primarily a function of the complex refractive index and particle volume. The particle volume can be estimated by measuring the mass with an APM and assuming a density. The scattering cross-section can be estimated from the elastic light scattering signal detected by the SP2. Using these two measurements and an assumed relationship between the real and imaginary parts of the refractive index, Moteki et al. determine the complex refractive index of ambient soot sampled in Tokyo, Japan. Although it is not clear how stringently the criteria of the Rayleigh-Gans approximation needs to be met, it appears the particle needs to be less than 300 nm in diameter for the analysis to be successful.

In this work, we present an approach for characterizing the absorption of single, non-spherical aerosol particles in the course-mode size range. This is an inaccessible parameter space using the techniques discussed above. Using a publicly available MSTM code [19], we calculate two-dimensional angular optical scattering (TAOS) patterns. The calculated TAOS patterns are meant to simulate TAOS patterns that can be captured by a previously described instrument [9]. We show that the size of the sphere clusters can be estimated by analyzing the size of the speckle in the simulated TAOS patterns. In addition, we explore how the integrated irradiance of the TAOS patterns, which correlates with the scattering cross-section, depends upon complex refractive index. Using the speckle-based measurement of particle size and approximate scattering cross-section from the integrated irradiance, we are able to distinguish between particles with various refractive indices from highly absorbing to non-absorbing over a size range of 2 μm to 10 μm. We conclude by discussing the limitations of our approach and the next steps for further validating the technique.

2. Background

The intensity and angular distribution of light scattered from an aerosol particle depend upon the particle size, shape, and composition. For example, it is well known that the scattering cross-section of a particle (i.e. the ratio between the radiant energy flux of light scattered by the particle and the incident irradiance) generally increases with particle size. Indeed, many particle sizing instruments are based on this property, such as products from Climet Instruments Company, Droplet Measurement Technologies, and TSI Incorprated. However, single-particle absorption can also affect the scattering cross-section [18, 20]. Thus, the scattering cross-section of an aerosol particle contains information about the absorptive properties of that particle as well as size.

A simple simulation conveys this dependence of the scattering cross-section on both particle size and absorption. Details about the simulation can be found in Section 3. Fig. 1(a) shows the backward- and forward-scattering hemispheres of a cluster of tightly packed spheres where the nominal diameter of the cluster is 8 μm and the wavelength of the incident light is 532 nm. The complex refractive index of the constituent spheres in the cluster is $1.53 + i\ 0$. By shrinking the cluster to a size of 5.6 μm, the scattering cross-section decreases by a factor of two. The scattering hemispheres of this small non-absorbing cluster are shown in Fig. 1(b). However, the same reduction in scattering cross-section can occur by changing the absorption of the particle rather than the cluster size. This can be done by keeping the diameter of the cluster at 8 μm but increasing the imaginary part of the refractive index of the constituent spheres from 0 to 0.1. The scattering hemispheres of this large, highly-absorbing cluster are shown in Fig. 1(c). This simple example displays a central idea in this paper. In particular, if the size of the particle is accounted for, insight into single-particle absorption can be discerned from elastic light scattering.

This example illustrates another central idea of this work. Looking closely at the scattering patterns in Fig. 1, the speckle in the scattering hemispheres increases in size and decreases in number as the cluster size shrinks from 8 μm

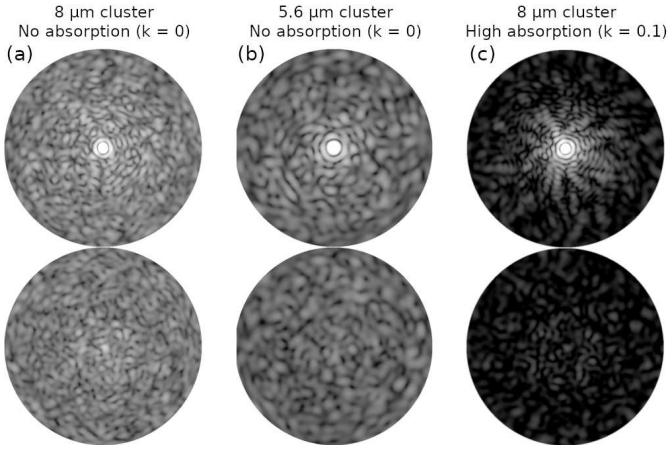

Figure 1: Simulated angular-resolved light scattering from sphere clusters. Each cluster is composed of 84 constituent spheres. Forward-scattering hemispheres (top row) and backward-scattering hemispheres (bottom row) are shown for (a) an 8 µm cluster of spheres with no absorption ($k = 0.0$), (b) a 5.6 µm small cluster of spheres with no absorption, and (c) an 8 µm cluster of spheres with high absorption ($k = 0.1$). To emphasize the features, a logarithmic scale is used for the brightness.

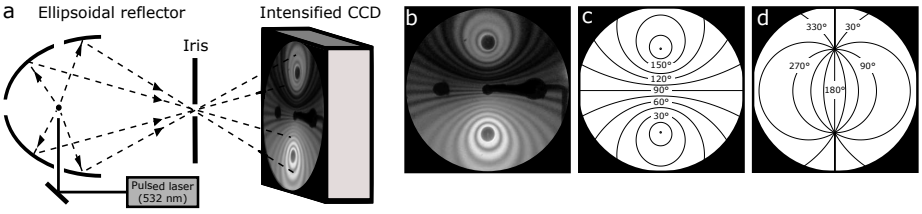

Figure 2: (a) Schematic of an apparatus that has been used to measure TAOS patterns [9]. The design allows for simultaneous measurement of the forward- and backward-scattering hemispheres from single aerosol particles. (b) A sample TAOS pattern measured from a spherical particle. (c) Polar coordinates mapped onto the detector plane. (d) Azimuthal coordinates mapped onto the detector plane.

to 5.6 μm. Multiple groups have noted and studied this effect [21, 22, 23, 24, 25, 26, 27]. For example, Ulanowski et al. explore the correlation between the average inverse area of the speckle and the aerosol nominal size [23]. Holler et al. show a correlation between the mean number of local peaks and valleys in intensity in the scattering pattern and the diameter of a cluster of spheres [21]. Brunel et al. estimate the dimensions of a particle by analyzing the central peak of the 2D-autocorrelation of the speckle pattern [26]. Thus the size of the particle, which affects the scattering cross-section, can be estimated from analysis of the speckle. By accounting for particle size by analyzing the speckle, the scattering cross-section can provide insight into the absorption of micron-sized nonspherical particles.

To further refine these ideas, we simulate the light-scattering patterns (i.e. TAOS patterns) collected by a previously realized instrument [9]. Fig. 2(a) shows a simplified diagram of the light-scattering collection optics. More details about the instrument are provided in previous published papers [9, 28]. By using an ellipsoidal mirror, a very large solid angle of scattered light can be detected spanning the polar scattering angle from 12° to 168° and the azimuthal scattering angle from 0° to 360°, although the experimental geometry significantly reduces the azimuthal coverage for certain polar angles. Fig. 2(b) depicts the captured TAOS pattern from a spherical particle. The polar and azimuthal scattering angles mapped onto the detector plane are shown in Fig. 2(c) and (d). The direction of the incident laser beam determines 0° for the polar scattering angle. The 0° for the azimuthal scattering angle is arbitrarily chosen. The dark black regions in the TAOS pattern are scattering angles not captured due to the instrument geometry. The forward- and backward-scattering hemispheres are estimated from the raw TAOS pattern by identifying the polar and azimuthal scattering angles associated with each pixel of the TAOS pattern and interpolating the irradiance of the forward- and backward-scattering hemispheres. The scattering hemispheres for two nonspherical particles are shown in Figure 3. Again, the dark black regions are scattering angles inaccessible by the experimental geometry. The scattering patterns from both particles have

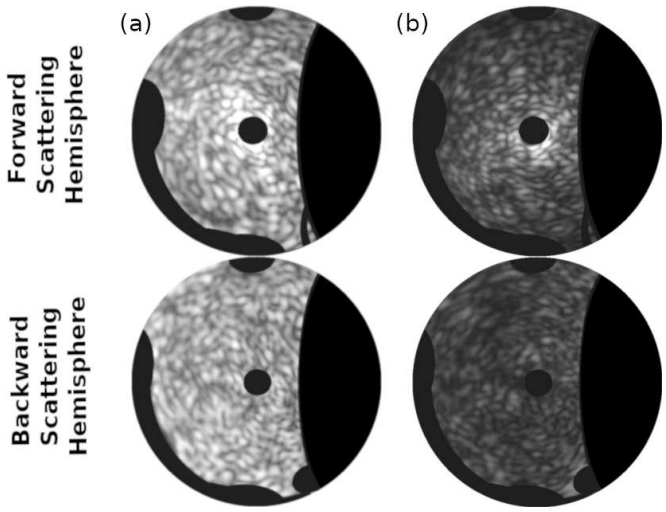

Figure 3: Experimentally captured TAOS patterns from two nonspherical particles plotted using spherical coordinates. The integrated irradiance of the light detected in (a) is six times larger than the light detected in (b). Note the speckle size seen in the two patterns is similar. A logarithmic scale is used to display the brightness.

similar speckle size, suggesting the particles are of similar size. However, the integrated irradiance (i.e. the sum of the photo-electron counts of all the pixels) of Figure 3(a) is six times larger than Figure 3(b). A possible interpretation of these findings is the particle that created the scattering pattern shown in Figure 3(b) was much more absorptive than the particle that created the scattering pattern shown in 3(a). By performing simulations that mimic the TAOS patterns captured by this instrument, we intend to explore this hypothesis and gain insight into how TAOS patterns can provide information about single-particle absorption.

3. Simulation and Speckle Analysis

Simulated TAOS patterns were calculated using Mackowski's publicly available MSTM Fortran code that calculates electromagnetic scattering and absorption properties of multiple sphere clusters [19, 29]. A position file containing the location and radius of each constituent sphere in the cluster is generated prior to

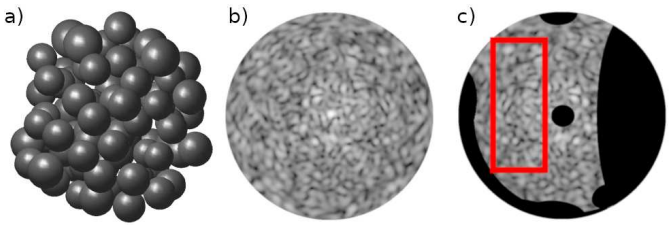

Figure 4: (a) Rendering of a simulated sphere cluster of nominal diameter 8 μm composed of 84 constituent spheres. (b) Calculated backward-scattering hemisphere resulting from illumination by a 532 nm wavelength plane wave. (c) Experimentally inaccessible light scattering angles are blacked out in the simulation to match experiment. The red box indicates the region used for 2D-autocorrelation analysis for speckle sizing.

running the MSTM code. The position file is generated by filling a sphere, set to the diameter of the cluster, with randomly generated points. These points represent the locations of the centers of the initial constituent spheres. Next, using the minimum diameter set for the constituent spheres, spheres are removed to prevent any overlap in volume. Finally, once all overlapping spheres have been removed, the radius of each constituent sphere is increased until it is about to touch the surface of another constituent sphere. This process results in a fairly tightly-packed sphere-like cluster with a very small distribution of constituent sphere diameters, as shown in Figure 4(a). The size range of the constituent spheres mimics that of spores or spore fragments [30].

The incident wavelength for the MSTM simulation was set to be 532 nm circularly polarized plane waves to match experimental conditions [9]. The value of the refractive index of the sphere clusters was varied to match four different particle types: oceanic, sulfate, dust, and soot [31, 32, 33]. These particle types provide a good range of values to test our technique and are physically relevant to aerosol optics. Table 1 displays the real and imaginary components of the refractive index for these four particle types. Using the MSTM code, the forward- and backward-scattering hemispheres are calculated for each simulated cluster. The backward-scattering hemisphere for the particle shown in 4(a) is displayed in 4(b). Finally, to mimic the experimental geometry,

Table 1: Complex refractive index of four particle types used in the simulations.

Particle Type	Complex Refractive Index
Oceanic	$1.38 + i\ 4.3 \times 10^{-9}$
Sulfate	$1.53 + i\ 7 \times 10^{-3}$
Dust	$1.53 + i\ 8 \times 10^{-3}$
Soot	$1.75 + i\ 0.43$

scattering angles that are inaccessible in the TAOS instrument are blacked out, as shown in 4(c).

As discussed in Section 2, the size of the particle can be estimated from the speckle in the TAOS patterns. The following procedure was used to determine the nominal size of the speckle from the simulated scattering patterns. Once the forward- and backward-scattering hemispheres were determined, the logarithm of the irradiance is calculated. Given the large dynamic range of elastic light scattering, using the logarithm of the irradiance improves analysis of the speckle features. The 2D-autocorrelation function of a subregion of the backward-scattering hemisphere is then calculated using MATLAB (The Mathworks Inc.) to determine the nominal speckle size. This subregion is indicated by a red rectangle in Fig4(c) and was chosen to both maximize the size of the region analyzed as well as avoid any scattering angles that are inaccessible to the experimental apparatus. Using the Image Processing Toolbox for MATLAB, the 2D-autocorrelation function is calculated and binarized with a threshold of 50% of the peak value. By performing the binarization, the central peak takes on a shape similar to an ellipse. Using the MATLAB *regionprops* function, the length (in pixels) of the major axis of the ellipse is determined. This value was then converted into an angular extent using the known conversion from pixels to degrees. This value, labeled $\Delta\theta$, serves as a measure of the nominal width of the speckle.

4. Results

A series of calculations were performed using the MSTM code to explore how speckle width and integrated irradiance varied with cluster properties such as the real and imaginary parts of the refractive index, the cluster diameter, the size of the constituent spheres of the cluster, as well as different configurations of a cluster. The starting point for the analysis was a cluster diameter of 6 μm with constituent spheres of minimum diameter of 0.945 μm and complex refractive index $1.53 + i\ 8 \times 10^{-3}$. The speckle width and integrated irradiance were calculated as each parameter was individually varied while keeping all other parameters constant.

Fig. 5(a) shows how the integrated irradiance and speckle width change for 10 different configurations of the constituent spheres. For each configuration, the position of the constituent spheres is different while the cluster diameter, the minimum constituent sphere size, and complex refractive index are held constant. The effect of varying the configuration of the constituent spheres has minimal impact on the integrated irradiance and speckle width. Both quantities appear to be fairly independent of constituent sphere configuration.

Next, the constituent sphere size is varied from 0.34 μm to 2 μm while keeping all other parameters constant. The integrated irradiance decreases, although not drastically, as shown in Fig. 5(b). The speckle width has limited variation. A similar procedure was followed to explore how the integrated irradiance and speckle width depend upon the real part of the refractive index. Again all cluster properties were kept constant except for the real part of the refractive index, which was varied from 1.3 to 2.0. The results, shown in Fig 5(c), are similar in magnitude as when the constituent sphere size is changed.

The imaginary part of the refractive index (k) is varied from 10^{-8} to 1 while keeping all other parameters constant. The results, displayed in Fig 5(d), show the speckle width remains fairly constant; whereas, integrated irradiance decreases by a factor of 7. Finally, the cluster diameter is varied from 1 μm to 10 μm while keeping all other parameters constant. The results are shown

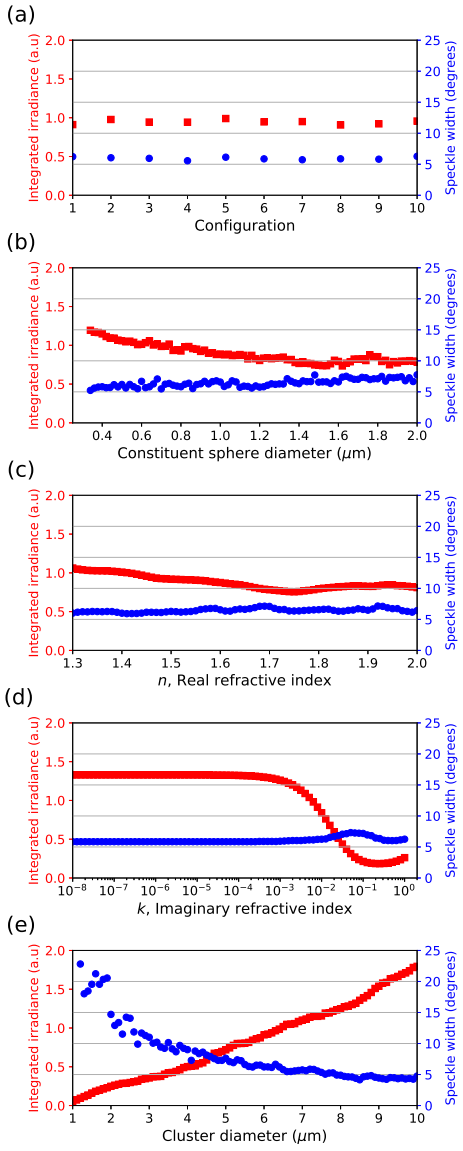

Figure 5: The speckle width and integrated irradiance were calculated as each parameter of a cluster was individually varied while keeping all other parameters constant. The starting point for the analysis was a cluster with a nominal diameter of 6 μm with constituent spheres of minimal diameter of 0.945 μm and complex refractive index $1.53 + i\ 8 \times 10^{-3}$. (a) The position of the constituent spheres is varied. (b) The minimal diameter of the constituent spheres is varied. (c) The real part of the refractive index is varied. (d) The imaginary part of the refractive index is varied. (e) The diameter of the cluster is varied.

in Fig 5(e). As expected, both the integrated irradiance and the speckle width vary greatly. The speckle width dramatically decreases from 20° to 4° over this change in cluster size while the integrated irradiance increases by more than a factor of 30.

From these results, we conclude the speckle width is independent or weakly dependent on all cluster properties except cluster diameter suggesting speckle width could be an excellent measure of cluster size. This agrees well with the work of other groups [23, 26, 27]. This result is not surprising as the speckle is caused by the change in phase of the light waves traversing the particle as well as the difference in pathlengths traversed by light rays from different parts of the particle to the detector plane. As the particle increases in size, this difference in pathlength undergo larger changes when the scattering angle is varied. The integrated irradiance, our experimental accessible proxy for scattering cross-section, significantly varies with both cluster diameter and the imaginary part of the refractive index of the constituent spheres.

Next, we explore whether we can differentiate between different particle types of aerosol particles, like oceanic sea-salt, sulfate, dust, and soot aerosols of differnt cluster sizes using the two experimentally accessible parameters of speckle width and integrated irradiance. Ideally, the speckle width solely depends upon the size of a cluster and no other particle properties. To check this, forward- and backward-scattering hemispheres are calculated using the MSTM code for various size clusters from 1 μm to 10 μm as well as 10 different configurations for each cluster. The complex refractive index of the constituent spheres is set to values given in Table 1. A total of 3,640 simulated TAOS patterns are calculated. The inverse of the speckle width is plotted as a function of cluster diameter. As shown in Fig. 6, the relationship appears to be linear, although the dynamic range is quite small. The correlation coefficient between the inverse of the speckle width and the cluster diameter is 0.98. All four particle types collapse onto a single curve indicating that indeed speckle width is primarily a function of cluster size, with only a minimal dependence on aerosol type. In performing a linear fit to the data, the relationship between speckle width in

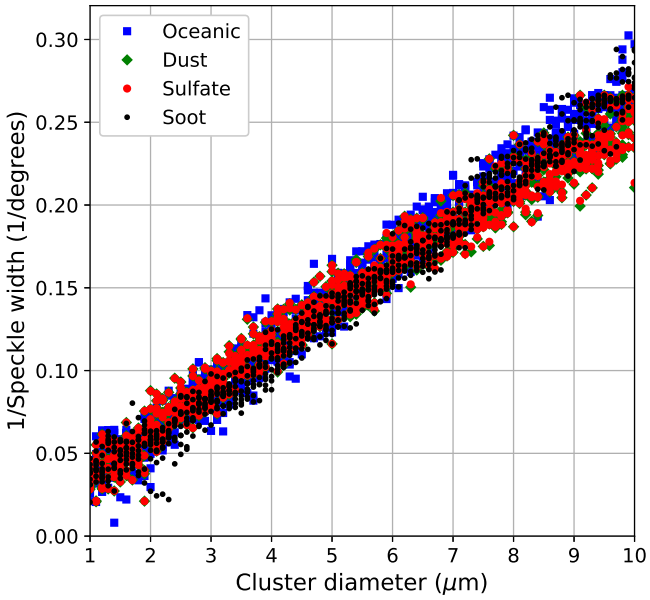

Figure 6: Relationship between particle cluster diameter and average speckle width. Results appear to be largely independent of particle composition.

degrees ($\Delta\theta$) and the cluster diameter in micrometers ($D_{cluster}$) is captured by the expression

$$\Delta\theta = 37.0/D_{cluster}. \quad (1)$$

The simulated TAOS data used to create Fig. 6 are further analyzed to explore whether the scattering patterns from different aerosol types, i.e. oceanic, dust, sulfate, and soot, can be distinguished from each other. In particular, for each simulated TAOS pattern, the cluster diameter is estimated from the speckle width and the integrated irradiance is calculated. By plotting these two quantities for all 3,640 simulated TAOS patterns, the different particle types separate as shown in Fig. 7. Highly absorbing soot particles have a much lower integrated irradiance than oceanic, dust, or sulfate particles of similar cluster size. Furthermore, non-absorbing oceanic particles have a slightly higher integrated irradiance than sulfate or dust particles. Sulfate and dust particles, which have

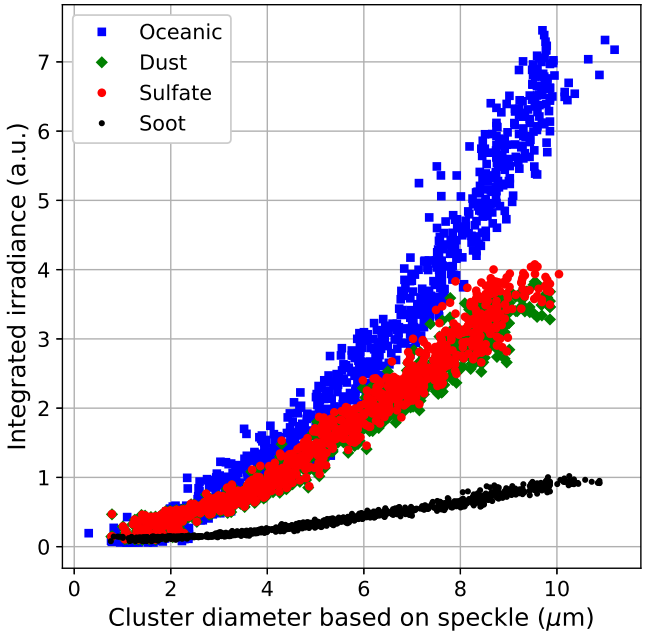

Figure 7: Graph of two experimentally accessible variables: Cluster diameter determined from the speckle width and the integrated irradiance of the scattering pattern. Highly absorbing clusters are clearly distinguishable from other clusters.

very similar complex refractive indices, are essentially indistinguishable from each other. As an example, for a 10 μm nominal diameter cluster, the integrated irradiance of a particle with optical properties similar to sulfate or dust is almost 4 times larger than a particle with optical properties similar to soot. The integrated irradiance of an oceanic particle is almost 7 times larger than that of soot. The separation between particle types diminishes as the cluster size is reduced. Below 6 μm in diameter, sulfate and dust data points become indistinguishable from oceanic data points. Below 2 μm, the data points for all four particles overlap. This result is not surprising if one considers that absorption should scale with particle volume, and thus elastic scattering from the smaller clusters should be more weakly dependent on the absorptive properties of the clusters.

Although Fig. 7 is promising and suggests that experimentally captured

TAOS patterns could be used to distinguish between particles with different absorption properties, further studies are needed. For example, all the simulated TAOS patterns for this work were calculated using the MSTM code. Thus, it is unclear how a change in particle morphology away from clusters of spheres would affect the analysis. However, Ulanowski et al. finds that speckle analysis is fairly robust in determining the size of particles of different origin and refractive index such as rough dust, smooth dust, a living cell, sphere clusters and a nearly smooth prismatic particle analogous to ice [23]. Clusters of spheres appear to depart somewhat from the general trend with a 30-40% reduction in speckle area.

Another challenge this approach faces is making absolute scattering intensity measurements by measuring the integrated irradiance of the detected TAOS pattern. Absolute intensity measurements are difficult and suffer from errors due to laser beam power and detector gain fluctuations, particle misalignment, and varying background levels. For example, the current instrument to capture TAOS patterns has fluctuations of integrated irradiance as large as a factor of 2 for monodispersed polystyrene spheres. This suggests that further modifications of the instrument are needed before detailed information can be gleaned from absolute scattering intensity measurements.

5. Summary

In this work, we present an approach for distinguishing between single non-spherical aerosol particles with varying absorptive properties in the course-mode size range. To test the approach, we simulated the TAOS patterns captured by a previously constructed instrument. Following the work of other groups, we found the speckle in the simulated TAOS patterns strongly correlates with the size of the aerosol particle, which is a sphere-like cluster for our simulation. In particular, the nominal width of the speckle ($\Delta\theta$) is related to the diameter of the cluster ($D_{cluster}$) by the expression $\Delta\theta = 37/D_{cluster}$. In addition, we found that the integrated irradiance of the TAOS pattern to have a strong

positive correlation with the size of the cluster and a negative correlation with the imaginary component of the refractive index of the constituent spheres in the cluster. With an independent measure of cluster size from the speckle, we show integrated irradiance can be used to distinguish between clusters that are strongly absorbing, weakly absorbing, and non-absorbing. This characterization becomes more difficult as the cluster size shrinks to 2 μm.

Acknowledgments

This work was supported by the U.S. Army Office, grant no. W911NF1420098. Thanks to Ronald G. Pinnick for collecting the TAOS images shown in Fig. 3 and to Daniel Landgraf for fruitful conversations and assisting in the creation of Fig. 2.

References

[1] T. C. Bond, S. J. Doherty, D. Fahey, P. Forster, T. Berntsen, B. DeAngelo, M. Flanner, S. Ghan, B. Kärcher, D. Koch, et al., Bounding the role of black carbon in the climate system: A scientific assessment, Journal of Geophysical Research: Atmospheres 118 (11) (2013) 5380–5552.

[2] I. N. Sokolik, O. B. Toon, Incorporation of mineralogical composition into models of the radiative properties of mineral aerosol from uv to ir wavelengths, Journal of Geophysical Research: Atmospheres 104 (D8) (1999) 9423–9444.

[3] M. Andreae, A. Gelencsér, Black carbon or brown carbon? the nature of light-absorbing carbonaceous aerosols, Atmospheric Chemistry and Physics 6 (10) (2006) 3131–3148.

[4] H. Moosmüller, R. Chakrabarty, W. Arnott, Aerosol light absorption and its measurement: A review, Journal of Quantitative Spectroscopy and Radiative Transfer 110 (11) (2009) 844–878.

[5] B. H. Samset, C. W. Stjern, E. Andrews, R. A. Kahn, G. Myhre, M. Schulz, G. L. Schuster, Aerosol absorption: Progress towards global and regional constraints, Current Climate Change Reports (2018) 1–19.

[6] S. Von Klot, J. Cyrys, G. Hoek, B. Kühnel, M. Pitz, U. Kuhn, B. Kuch, C. Meisinger, A. Hörmann, H.-E. Wichmann, et al., Estimated personal soot exposure is associated with acute myocardial infarction onset in a case-crossover study, Progress in Cardiovascular Diseases 53 (5) (2011) 361–368.

[7] B. Weinhold, Global bang for the buck: Cutting black carbon and methane benefits both health and climate, Environmental Health Perspectives 120 (6) (2012) a245.

[8] B. J. Mason, S.-J. King, R. E. Miles, K. M. Manfred, A. M. Rickards, J. Kim, J. P. Reid, A. J. Orr-Ewing, Comparison of the accuracy of aerosol refractive index measurements from single particle and ensemble techniques, The Journal of Physical Chemistry A 116 (33) (2012) 8547–8556.

[9] K. B. Aptowicz, Y.-L. Pan, S. D. Martin, E. Fernandez, R. K. Chang, R. G. Pinnick, Decomposition of atmospheric aerosol phase function by particle size and asphericity from measurements of single particle optical scattering patterns, Journal of Quantitative Spectroscopy and Radiative Transfer 131 (2013) 13–23.

[10] R. E. Willoughby, M. I. Cotterell, H. Lin, A. J. Orr-Ewing, J. P. Reid, Measurements of the imaginary component of the refractive index of weakly absorbing single aerosol particles, The Journal of Physical Chemistry A 121 (30) (2017) 5700–5710.

[11] M. Nakagawa, T. Nakayama, H. Sasago, S. Ueda, D. S. Venables, Y. Matsumi, Design and characterization of a novel single-particle polar nephelometer, Aerosol Science and Technology 50 (4) (2016) 392–404.

[12] Z. Gong, Y.-L. Pan, C. Wang, Characterization of single airborne particle extinction using the tunable optical trap-cavity ringdown spectroscopy (ot-crds) in the uv, Optics Express 25 (6) (2017) 6732–6745.

[13] N. Oshima, Y. Kondo, N. Moteki, N. Takegawa, M. Koike, K. Kita, H. Matsui, M. Kajino, H. Nakamura, J. Jung, et al., Wet removal of black carbon in asian outflow: Aerosol radiative forcing in east asia (a-force) aircraft campaign, Journal of Geophysical Research: Atmospheres 117 (D3).

[14] J. D. Allan, W. T. Morgan, E. Darbyshire, M. J. Flynn, P. I. Williams, D. E. Oram, P. Artaxo, J. Brito, J. D. Lee, H. Coe, Airborne observations of iepox-derived isoprene soa in the amazon during sambba, Atmospheric Chemistry and Physics 14 (20) (2014) 11393–11407.

[15] M. Stephens, N. Turner, J. Sandberg, Particle identification by laser-induced incandescence in a solid-state laser cavity, Applied Optics 42 (19) (2003) 3726–3736.

[16] J. Schwarz, R. Gao, D. Fahey, D. Thomson, L. Watts, J. Wilson, J. Reeves, M. Darbeheshti, D. Baumgardner, G. Kok, et al., Single-particle measurements of midlatitude black carbon and light-scattering aerosols from the boundary layer to the lower stratosphere, Journal of Geophysical Research: Atmospheres 111 (D16).

[17] N. Moteki, Y. Kondo, Effects of mixing state on black carbon measurements by laser-induced incandescence, Aerosol Science and Technology 41 (4) (2007) 398–417.

[18] N. Moteki, Y. Kondo, S.-i. Nakamura, Method to measure refractive indices of small nonspherical particles: Application to black carbon particles, Journal of Aerosol Science 41 (5) (2010) 513–521.

[19] D. W. Mackowski, M. I. Mishchenko, Calculation of the t matrix and the scattering matrix for ensembles of spheres, JOSA A 13 (11) (1996) 2266–2278.

[20] K. B. Aptowicz, Y.-L. Pan, R. K. Chang, R. G. Pinnick, S. C. Hill, R. L. Tober, A. Goyal, T. Jeys, B. V. Bronk, Two-dimensional angular optical scattering patterns of microdroplets in the mid infrared with strong and weak absorption, Optics Letters 29 (17) (2004) 1965–1967.

[21] S. Holler, Y.-L. Pan, R. K. Chang, J. R. Bottiger, S. C. Hill, D. B. Hillis, Two-dimensional angular optical scattering for the characterization of airborne microparticles, Optics Letters 23 (18) (1998) 1489–1491.

[22] S. Holler, S. Zomer, G. F. Crosta, Y.-L. Pan, R. K. Chang, J. R. Bottiger, Multivariate analysis and classification of two-dimensional angular optical scattering patterns from aggregates, Applied Optics 43 (33) (2004) 6198–6206.

[23] Z. Ulanowski, E. Hirst, P. H. Kaye, R. Greenaway, Retrieving the size of particles with rough and complex surfaces from two-dimensional scattering patterns, Journal of Quantitative Spectroscopy and Radiative Transfer 113 (18) (2012) 2457–2464.

[24] Z. Ulanowski, P. H. Kaye, E. Hirst, R. Greenaway, R. J. Cotton, E. Hesse, C. T. Collier, Incidence of rough and irregular atmospheric ice particles from small ice detector 3 measurements, Atmospheric Chemistry and Physics 14 (3) (2014) 1649–1662.

[25] R. Fu, C. Wang, O. Muñoz, G. Videen, J. L. Santarpia, Y.-L. Pan, Elastic back-scattering patterns via particle surface roughness and orientation from single trapped airborne aerosol particles, Journal of Quantitative Spectroscopy and Radiative Transfer 187 (2017) 224–231.

[26] M. Brunel, H. Shen, S. Coëtmellec, G. Gréhan, T. Delobel, Determination of the size of irregular particles using interferometric out-of-focus imaging, International Journal of Optics 2014.

[27] M. Talbi, G. Grehan, M. Brunel, Interferometric particle imaging of ice

particles using a multi-view optical system, Applied Optics 57 (21) (2018) 6188–6197.

[28] G. E. Fernandes, Y.-L. Pan, R. K. Chang, K. Aptowicz, R. G. Pinnick, Simultaneous forward-and backward-hemisphere elastic-light-scattering patterns of respirable-size aerosols, Optics Letters 31 (20) (2006) 3034–3036.

[29] D. Mackowski, M. Mishchenko, A multiple sphere t-matrix fortran code for use on parallel computer clusters, Journal of Quantitative Spectroscopy and Radiative Transfer 112 (13) (2011) 2182–2192.

[30] A. M. Madsen, S. T. Larsen, I. K. Koponen, K. I. Kling, A. Barooni, D. G. Karottki, K. Tendal, P. Wolkoff, Generation and characterization of indoor fungal aerosols for inhalation studies, Applied and Environmental Microbiology (2016) AEM–04063.

[31] M. A. Box, G. P. Box, Physics of Radiation and Climate, CRC Press, 2015.

[32] A. A. Kokhanovsky, Aerosol Optics: Light Absorption and Scattering by Particles in the Atmosphere, Springer Science & Business Media, 2008.

[33] C. Levoni, M. Cervino, R. Guzzi, F. Torricella, Atmospheric aerosol optical properties: a database of radiative characteristics for different components and classes, Applied Optics 36 (30) (1997) 8031–8041.